# Dynamic perineuronal net expression during learned maternal behavior is cortical hemisphere-specific and dependent on methyl-CpG-binding protein 2

Billy Y.B. Lau, Dana E. Layo, Brett Emery, Matthew Everett, Anushree Kumar, Parker Stevenson, Kristopher G. Reynolds, Andrew Cherosky, Sarah-Anne H. Bowyer, Sarah Roth, Delaney Fisher, Rachel P. McCord, Keerthi Krishnan

Cortical neuronal circuits along the sensorimotor pathways are shaped by experience during critical periods of heightened plasticity in early postnatal development. After closure of critical periods, measured histologically by the formation and maintenance of extracellular matrix structures called perineuronal nets (PNN), the adult mouse brain exhibits restricted plasticity and maturity. Mature PNN are typically considered to be stable structures that restrict synaptic plasticity on cortical parvalbumin+ GABAergic neurons. However, changes in environment, such as novel behavioral training or social contexts such as motherhood, elicit synaptic plasticity in relevant neural circuitry. Currently, it is unclear if extracellular matrix plasticity, as measured by PNN density, occurs in such social contexts in adult wildtype female mice. Here, we found novel PNN density changes in the primary somatosensory cortex (SS1) in a hemisphere-, subregion- specific manner after a maternal behavior task, using systematic whole brain region microscopy analysis. Furthermore, we found hemispheric bias in PNN density in individual mice. Using adult female mice deficient in methyl-CpG-binding protein 2 (MECP2), an epigenetic regulator, we found that MECP2 is critical for this precise and dynamic expression of PNN.

**Abbreviations:**

PNN - Perineuronal nets
WFA – Wisteria Floribunda Agglutinin
PV+ - Parvalbumin+ GABAergic neurons
MECP2 – Methyl CpG-binding protein 2
NW – Naïve wild type
NH – Naïve *Mecp2* heterozygote
SW – Surrogate wild type
SH – Surrogate *Mecp2* heterozygote
PCA – Principal component analysis

SS1 – Primary somatosensory cortex
Subregions of SS1:
S1BF – barrel cortex
S1DZ – dysgranular zone
S1FL – Forelimb region
S1J – Jaw region
S1ULp – Upper lip
S1Tr – Trunk region
S1HL – Hind limb
S1 – Undefined somatosensory cortex

Department of Biochemistry & Cellular and Molecular Biology, University of Tennessee, Knoxville, TN 39996
**Corresponding author**: Dr. Keerthi Krishnan, (865) 974-4157, krishnan@utk.edu

**Introduction:**

Perineuronal nets (PNNs) are specialized extracellular matrix structures that can act as physical barriers or modulators of plasticity, restrict axon regeneration, and form molecular brakes that actively control synaptic maturation and the function of cortical parvalbumin+ (PV+) GABAergic interneurons that drive gamma oscillations (Bartos et al., 2002; Begum and Sng, 2017; Bernard and Prochiantz, 2016; Carstens et al., 2016; Deepa et al., 2002; Dityatev et al., 2007; Donato et al., 2013; Durand et al., 2012; Frischknecht et al., 2009; Gundelfinger et al., 2010; Hartig et al., 1992; Hou et al., 2017; Kalemaki et al., 2018; Kosaka and Heizmann, 1989; Krishnan et al., 2015, 2017; Nakagawa et al., 1986; Orlando et al., 2012; Pizzorusso et al., 2002, 2006; Sigal et al., 2019; Sugiyama et al., 2009; Suttkus et al., 2012; Ueno et al., 2018; Vo et al., 2013; de Winter et al., 2016; Ye and Miao, 2013). Mature PNNs in the adult cortices are thought to be stable structures, inhibitory to plasticity, and perhaps play roles in long term memory such as “engrams” (Carstens et al., 2016; Gogolla et al., 2009; Thompson et al., 2018). However, most of these observations are based on postnatal cortical development (when typical connections in neural circuitry are still forming) and models for neurobiological disorders (where neural circuitry development and function have gone awry). Currently, it is unclear if changes in adult PNN density occur under normal conditions and behavioral contexts.

PNNs are composed of chondroitin sulfate proteoglycans, hyaluronan glycosaminoglycan chains, Link proteins and Tenascin-R (Bignami et al., 1992; Carulli et al., 2007; Kwok et al., 2010; Miyata and Kitagawa, 2017). Wisteria floribunda agglutinin (WFA), which specifically binds to N-acetyl galactosamine found on most chondroitin sulfate side chains on chondroitin sulfate proteoglycans, is commonly used as a marker for PNNs in the cortex and other brain regions (Brückner et al., 1996; Hartig et al., 1992). PNNs are localized predominantly around soma and proximal dendrites of parvalbumin+ GABAergic interneurons of the mature cortex. They interdigitate with synaptic contacts on cortical PV+ GABAergic neurons and regulate experience-dependent synaptic plasticity in the cortex, hippocampus and amygdala (Cattaud et al., 2018; Gogolla et al., 2009; Krishnan et al., 2015, 2017; Miyata et al., 2012; Murthy et al., 2019; Sigal et al., 2019).

In the human brain, decreased numbers of PNNs are associated with pathological conditions such as decreased memory and motor agility (Brückner et al., 2008; Morawski et al., 2004). Mouse models for varying neurological disorders show abnormal/atypical expression of PNNs which, when removed, can greatly improve the associated pathology or behavioral readouts in these models (Berretta et al., 2015; Krishnan, Lau et al., 2017; Pizzo et al., 2016; Reinhard et al., 2019). We have previously shown that precocious or atypical expression of PNNs caused sensory processing deficits in developing male and adult female mouse models for Rett Syndrome, respectively (Krishnan et al., 2015, 2017). Rett Syndrome is a neuropsychiatric disorder predominantly caused by mutations in the X-linked gene, methyl CpG-binding protein 2 (MECP2) (Amir et al., 1999). MECP2 regulates neuronal chromatin architecture and gene transcription in response to neural activity and experience during postnatal life (Becker et al., 2016; Chahrour et al., 2008; Ebert et al., 2013; Skene et al., 2010; Zhou et al., 2006). The known cellular function of MECP2 and the characteristic timing of disease progression led us to hypothesize that MECP2 regulates experience-dependent plasticity in specific neural circuits during windows of enhanced sensory and social experience throughout life; disruptions in timing of these plasticity mechanisms results in atypical responses in behavior. We previously tested this hypothesis using a pup retrieval task in the maternal behavior paradigm (Krishnan, Lau et al., 2017).

Parenting is an ethologically relevant social behavior consisting of stereotypic components involving the care and nourishment of young. First-time dams seek and gather wandering/scattered pups back to the nest (pup retrieval), an essential aspect of maternal care. Pup retrieval involves processing of primary sensory cues (auditory, tactile, olfactory) to direct efficient searching and gathering of pups with goal-directed movements back to the nest (Beach and Jaynes, 1956; Lonstein et al., 2015; Stern, 1996). Virgin female mice with no previous maternal experience (‘surrogates’ or ‘Sur’) can execute efficient pup retrieval after co-housing with a first-time mother and her pups (Cohen

et al., 2011a). This assay allows for interrogation of adult experience-dependent plasticity mechanisms (and likely non-hormonal epigenetic mechanisms involving the sensory and motor neural circuits (Stolzenberg and Champagne, 2016).

Previously, we found that atypical increase in PNN density in the auditory cortex of *Mecp2*-heterozygous females caused inefficient pup retrieval (Krishnan, Lau et al., 2017). However, we did not find discernable changes in PNN density in the wildtype auditory cortex after successful completion of the pup retrieval task. On the one hand, as PNNs were considered as barriers to plasticity, we anticipated reduction in PNN density in wildtype that could facilitate efficient retrieval. On the other hand, there are no known reports of reduction in PNN expression in normal adult wildtype brains. Here, we seek to answer if mature PNNs are maintained as stable structures or undergo changes in expression in the primary somatosensory cortex (SS1) of adult female mice. We focused on the SS1 due to its known roles in tactile sensation, which is also important for efficient pup retrieval (Brecht, 2007; Feldman and Brecht, 2005; Kenyon et al., 1981; Morgan et al., 1992). By using WFA as a marker in this whole-brain systematic analysis of SS1, we find that PNNs 1) are differentially expressed in a hemisphere-specific, subregion-specific manner, 2) show dynamic changes in density after behavioral exposure, and 3) are influenced by MECP2, a DNA methylation reader/epigenetic regulator of chromatin and gene expression.

**Materials and Methods:**

Animals:

All experiments were performed in adult female mice (10-12 weeks old) that were maintained on a 12hr light-dark cycle (lights on 07:00 h) and received food ad libitum. Genotypes used were CBA/CaJ, *MeCP2*$^{Het}$ (C57BL/6 background; B6.129P2(C)-*Mecp2*$^{tm1.1Bird}$/J) and *MeCP2*$^{WT}$ (Guy et al., 2001). All procedures were conducted in accordance with the National Institutes of Health's Guide for the Care and Use of Laboratory Animals and approved by the University of Tennessee-Knoxville Institutional Animal Care and Use Committee.

Pup retrieval behavior:

Pup retrieval behavior was performed as previously described (Krishnan, Lau et al., 2017). Briefly, we housed two virgin female mice (one *MeCP2*$^{WT}$ and one *MeCP2*$^{Het}$ termed 'surrogates', SW and SH respectively) with a first-time pregnant CBA/CaJ female beginning 1-5 days before birth. Pup retrieval behavior started on the day the pups were born (postnatal day 0; D0) as follows for each adult surrogate mouse: 1) (habituation phase) one adult mouse was habituated with 3-5 pups in the home cage for 5 minutes, 2) (isolation phase) pups were removed from the cage for 2 minutes, and 3) (retrieval phase) pups were returned to home cage, one placed at each corner and at the center (the nest was left empty if there were fewer than 5 pups). Each adult female had maximum of 10 minutes to gather the pups to the original nest. After testing, all animals and pups were returned to the home cage. The same procedure was performed again daily to D5. All behaviors were performed in the dark, during the light cycle (between 9:00 AM and 6:00 PM) and were video recorded.

Immunohistochemistry:

Immediately after the behavioral trial on D5, surrogate mice as well as a set of corresponding nulliparous Naïve WT and Het (NW and NH, respectively) mice were perfused with 4% paraformaldehyde/PBS, and brains were extracted and post-fixed overnight at 4°C. Brains were then treated with 30% sucrose/PBS overnight at room temperature (RT) and microtome- sectioned in sagittal orientation at 70µm. Free-floating brain sections were immunostained at RT as previously described in Krishnan, Lau et al., 2017, with a few modifications. Briefly, sections were blocked in 10% normal goat serum and 0.5% Triton-X for 3 hours, then incubated with biotin-conjugated Wisteria Floribunda Agglutinin Lectin (labels PNNs; 1:500; Sigma-Aldrich) overnight in a 5% normal goat serum/0.25% Triton-X solution. Then, sections were incubated for 4 hours with AlexaFluor-488 secondary antibody in a 5% normal goat serum/0.25% Triton-X solution: (1:1000; Invitrogen). Finally, sections were

counterstained with the nuclear marker, DAPI (1:1000) for 5 minutes, and mounted in Fluoromount-G (Southern Biotech).

Image acquisition and analysis:
To analyze PNNs, 10X single-plane PNN images of the entire primary somatosensory cortex from each brain slice were acquired on a motorized stage, epifluorescent microscope (Keyence BZ-X710; Keyence Corp., NJ, U.S.A.) and stitched using BZ-X Analyzer (Keyence). Our initial observation of PNN intensity showed that SH had the most intense fluorescent signal in SS1. Thus, imaging settings were established based on SH within each cohort of mice, in order to minimize over-exposure. The light exposure time for fluorescent signal acquisition was identified by finding the exposure time where a saturated pixel first appears within frame, then decreasing the exposure time by 1 unit, according to software specifications. This exposure time determination method was applied to all brain sections of SH in each cohort and the mean exposure time was calculated and used for final image acquisition within each cohort.

For image analysis, each stitched image was opened in ImageJ (Schneider et al., 2012). Then, SS1 and somatosensory subregion areas were 1) mapped by overlaying templates from Paxinos and Franklin's "The Mouse Brain, 4$^{th}$ edition", 2) outlined and 3) measured using the functions in ImageJ (Paxinos and Franklin, 2013). To count high-intensity mature PNNs, the 'Contrast' setting from the browser was set to the far right to threshold weaker signals. The remaining signals were manually quantified under the classification that a 'mature' PNN is at least 80% of its original shape (before contrast adjustment). All statistical analyses and graphs were generated using either GraphPad Prism.

Principal Components Analysis (PCA) on PNN density:
We used raw PNN densities (counts per area) for the entire SS1 across all individuals in the five cohorts. If multiple sections per map number (according to the atlas, reported as bregma values in this paper) were present, values were averaged across sections to give a single density. In the first PCA analysis, to determine whether the PNN patterns segregated primarily by cohort or according to condition (genotype and experience), we kept the data for each individual animal separate and averaged PNN densities across every set of 2 adjacent map regions. Because the scale of raw numbers varied so widely between individual animals, we next median normalized PNN densities within each animal. Some regions for some individuals had no data, and, because PCA does not tolerate missing data, we imputed these missing values by using the average median normalized values for that region from animals in other cohorts in the same condition. By running PCA in R, we obtained a weight for each map number showing the highest variance patterns in PNN densities across the individual animals. We then calculated the projection of each animal onto principle components 1 and 2. K-means clustering was used to calculate the two most evident clusters in this PCA space.
In the second PCA analysis, to determine the major PNN density patterns that distinguish genotypes and experience conditions, we left data for each map number separate, but averaged the median normalized PNN densities across the 5 cohorts for each condition. We then performed PCA to determine the major patterns that distinguish these conditions.

## Results:

### Changes in PNN density across somatosensory cortical maps:

The somatosensory cortex encompasses the largest region by area of the mouse cortex. According to Paxinos and Franklin's atlas (4$^{th}$ edition), there are eight different anatomical somatosensory cortical subregions (S1, S1BF, S1DZ, S1FL, S1J, S1ULp, S1Tr and S1HL), here collectively called primary somatosensory cortex (SS1) (Paxinos and Franklin, 2013). To determine how PNN expressions are changing across the different SS1 subregions, we took a systematic approach covering the whole SS1, rather than the standard approach of analyzing "representative sample sections". We analyzed 40-60 sagittal brain sections (at 70um each, both left and right hemispheres) per animal, in five biological replicates across four conditions (two genotypes: one

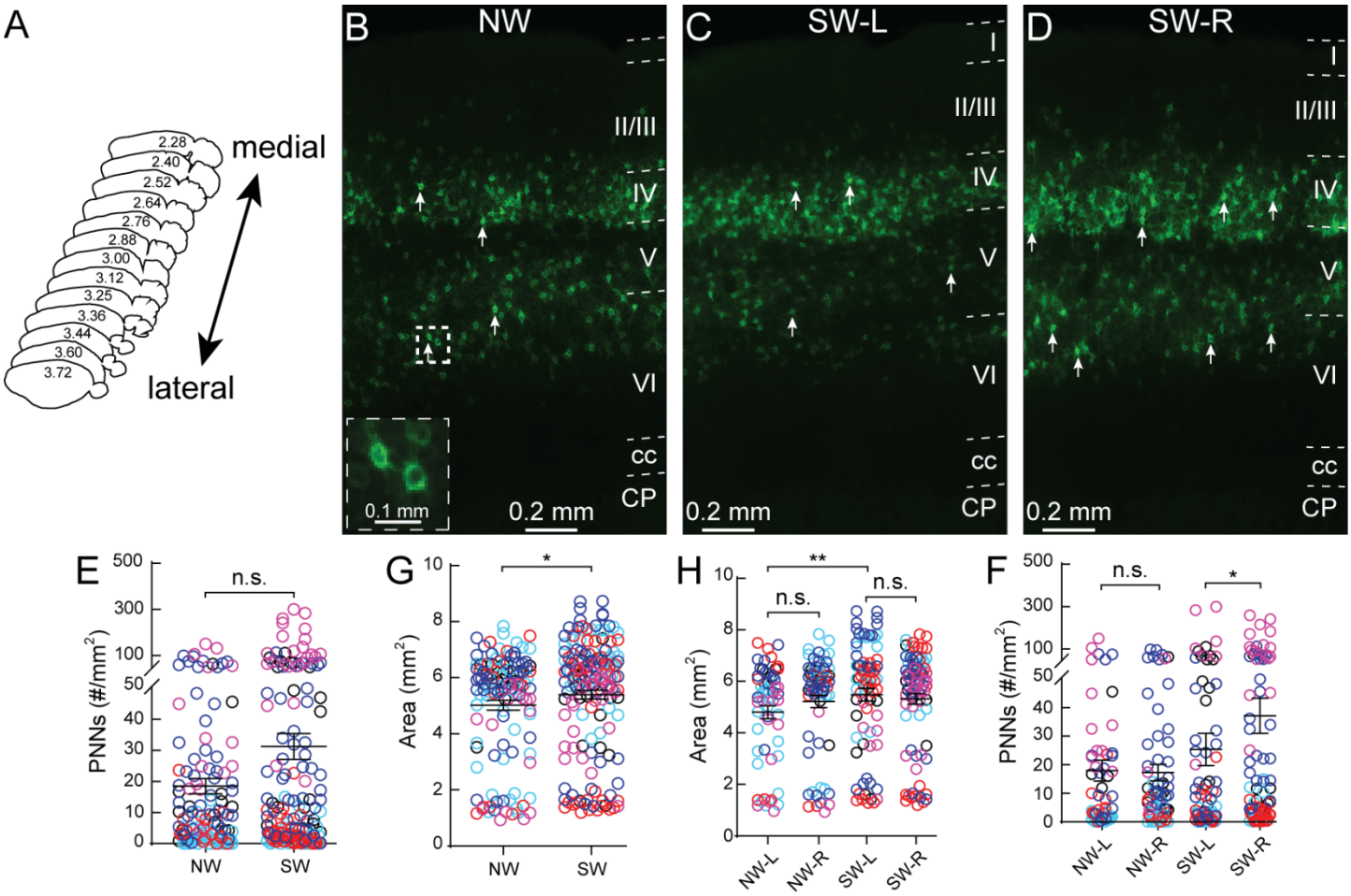


**Figure 1: *Mecp2$^{WT}$* (*Wildtype*) mice exhibit hemisphere specific increase in PNN density in the primary somatosensory cortex (SS1) after maternal behavior. (A)** Schema of mouse brain sections cut in sagittal orientation, depicting all medial (2.28 mm, corresponding to map number 120) to lateral (3.72 mm, corresponding to map number 132) regions of SS1 analyzed for this study. Coordinate maps are based on Paxinos and Franklin's mouse brain atlas, 4th edition. (**B-D**) Representative epifluorescent images of PNN expression in SS1 of Naïve WT (NW) (B) as well as left (L) (C) and right (R) (D) hemispheres of Surrogate WT (SW). Layers 1 through 6 are outlined. CP = caudate putamen and cc = corpus callosum. Arrows indicate high-intensity PNNs analyzed for the study. Inset in B shows 2 high-intensity PNNs. **(E)** Combined hemispheres' analysis of the density of high-intensity PNNs was not significantly different between NW and SW (NW: n = 123 images; SW: n = 162; *Mann-Whitney test, $p > 0.05$*). **(F)** Separate analysis of left and right hemispheres revealed a significant increase of high-intensity PNNs in the right hemisphere of SW (SW-R; n = 81 images) compared to the left hemisphere of SW (SW-L; n = 81 images) (*Kruskal-Wallis followed by Dunn's test, *$p < 0.05$*), while no significant difference was observed between hemispheres of NW (NW-L: n = 59 images; NW-R: n = 64 images; *Mann-Whitney test, $p > 0.05$*). (**G-H**) Size of SS1 was overall significantly larger in SW compared to NW (G) (NW: n = 123 images; SW: n = 162 images). Enlargement of SS1 in SW occurred in the left hemisphere (H) (NW-L: n = 59 images, NW-R: n = 64 images; SW-L: n = 81 images; SW-R: n = 81 images; *Kruskal-Wallis followed by Dunn's test, **$p < 0.01$*). For E-H, n.s. = not significant. Different colors represent each of the five cohorts. Each open circle represents PNN density in an individual brain section.

experienced surrogate, one naïve), as qualitative regional differences in PNN density was observed in pilot studies in our lab. As somatosensation during pup retrieval primarily involves facial/snout areas in surrogates (non-lactating adult females) (Lonstein et al., 1997; Morgan et al., 1992; Paxinos and Franklin, 2013; Stern, 1996), we present data collected from map numbers 120-132, corresponding to 2.28 mm (medial) to 3.72 mm (lateral) regions (Figure 1A), which encompasses ~1.5 mm of the mouse brain.

Across the five cohorts, PNN density (as measured by high-intensity PNN counts over area) was not significantly different between Naïve WT (NW) and Surrogate WT (SW) across the SS1 (Figure 1E). However, we noticed differences in PNN density per section across cohorts, ranging from 1 to 300. In order to determine the source of such variability, we parsed the data according to hemispheres (Figure 1F), across the lateral-medial axis (Figure 2) and subregions (Figure 3). No significant

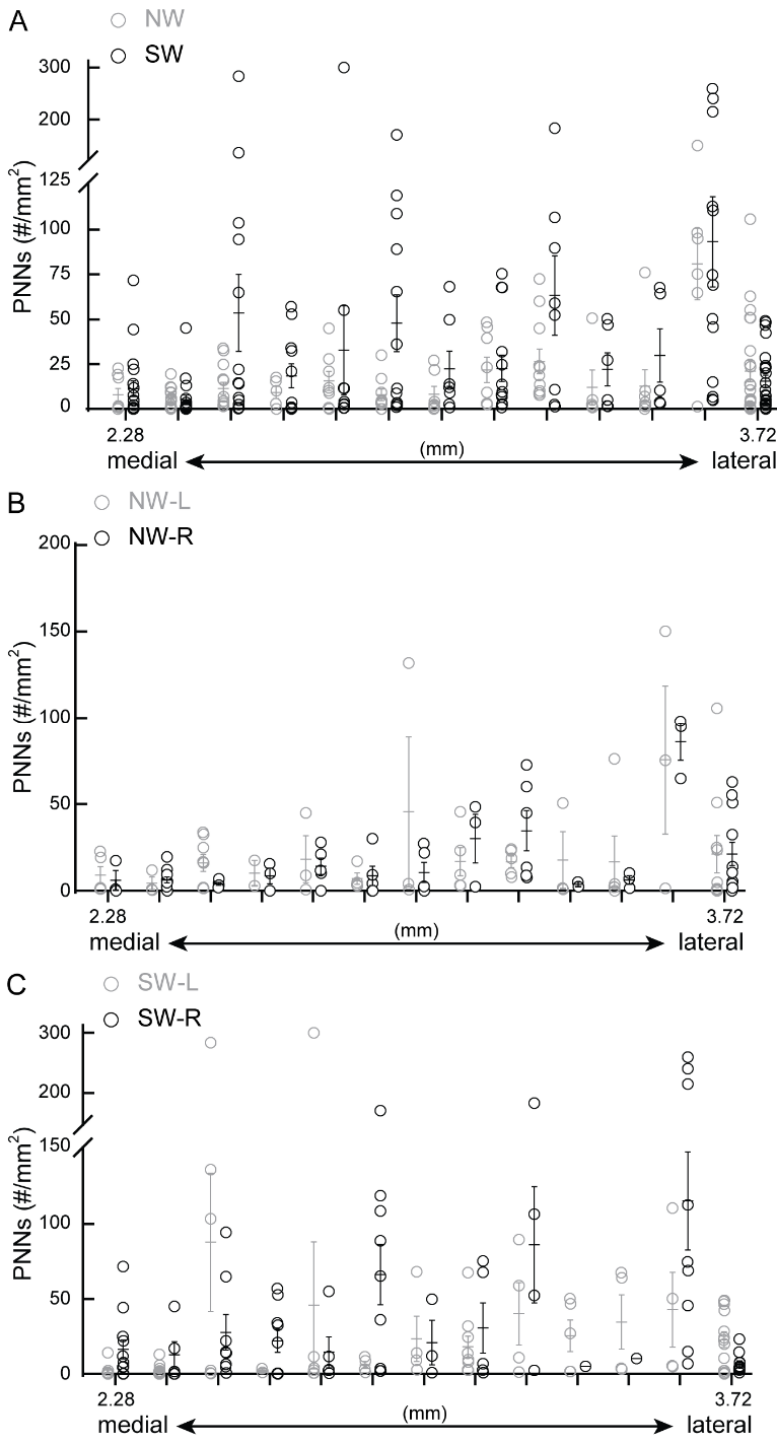


**Figure 2: Dynamic changes in PNN density across medial/lateral axis before and after maternal experience. (A)** Mean distribution of combined PNN density from left and right hemispheres of SS1 revealed a gradual increase of PNN density from medial (starting at 2.28 mm) to lateral (ends at 3.72 mm) SS1 in NW. After maternal experience, SW exhibited an increased PNN density throughout SS1. N = 5 – 24 images per region, 5 mice per condition. **(B)** In NW, the mean distribution of PNN density was similar between left and right hemispheres throughout SS1. **(C)** SW exhibited dynamic changes in PNN density between left and right hemispheres as well as throughout medial and lateral SS1. For A-C, mean ± S.E.M. are shown. Each dot represents PNN density in an individual section. 5 mice per condition. For B and C, n = 1 – 13 images per map coordinate.

difference was observed in PNN density between the left and right hemispheres of NW; however, the right hemisphere of SW (SW-R) had increased PNN density compared to the left hemisphere (SW-L) (Figure 1F), suggesting that learned maternal experience contributes to increased PNN density in the right hemisphere of SS1, possibly to consolidate new tactile information related to the pups and/or the mother.

As PNN density is dependent on area, we noticed that overall SS1 area of the SW is significantly increased, compared to NW (Figure 1G); however, that increase was not specific to a particular hemisphere within experimental condition (NW-L vs. NW-R; SW-L vs. SW-R) (Figure 1H). After experience, there is a small but significant area increase in left hemisphere, shown also in Figure 1H.

Next, we plotted PNN density in individual sections across the lateral-medial axis (Figure 2). The lateral sections of SS1, past bregma 3.5 mm, had a consistently higher density of PNNs compared to the medial sections, in both NW and SW. However, changes in PNN density after surrogacy experience was seen in more medial sections (Figure 2A). NW had similar PNN density across left (grey) and right (black) hemispheres (Figure 2B), while SW showed hemisphere-specific changes in PNN density (previously observed in Figure 1F) across the lateral-medial axis (Figure 2C).

**Changes in PNN density are subregion-specific:**

Next, we examined if specific subregions were particularly plastic for PNN density between NW and SW. We observed no significant differences in PNN density in subregions S1BF, S1DZ and S1FL using both hemispheres (Figure 3A - C). We found significant differences between hemispheres after surrogacy in S1DZ (Figure 3B') and S1FL (Figure 3C') with greater PNN density in

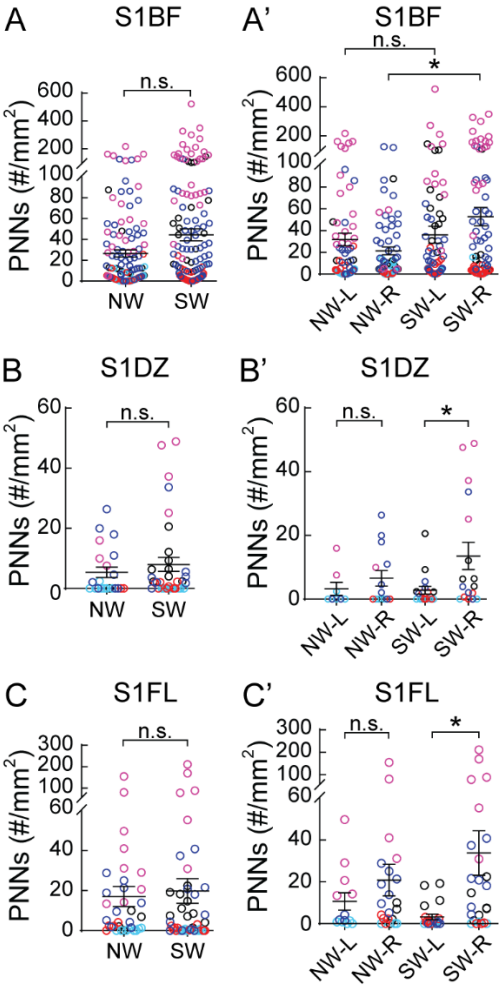


**Figure 3: PNN density varies across subregions of SS1. (A-C)** Analysis of both hemispheres for SS1 barrel field (S1BF, A), dysgranular zone (S1DZ, B) and forelimb (S1FL, C) revealed no significant differences between NW and SW (S1BF: NW - n = 131 images, SW - n = 168 images; S1DZ: NW – n = 22 images, SW – n = 35 images; S1FL: NW – n = 35 images, SW – n = 46 images; 5 mice per condition; *Mann-Whitney test, p > 0.05, n.s. = not significant*). **(A'-C')** Analysis of subregional SS1 by hemispheres revealed dynamic changes in PNN expression. In S1BF (**A'**), a significant increase of PNN expression was detected in the right hemisphere of SW (SW-R) compared to NW (NW-R) (NW-L: n = 65 images; NW-R: n = 66 images; SW-L: n = 85 images; SW-R: n = 83 images; 5 mice per condition; *Kruskal-Wallis followed by Dunn's test, *p < 0.05*). In S1DZ (**B'**), while no significant difference was observed in PNN density between hemispheres in NW, maternal experience significantly increased PNN density in the right hemisphere (SW-R) compared to the left (SW-L) (NW-L: n = 8 images; NW-R: n = 14 images; SW-L: n = 18 images; SW-R: n = 17 images; 5 mice per condition; *Kruskal-Wallis followed by Dunn's test, *p < 0.05*). A similar pattern of PNN plasticity was also detected in S1FL (**C'**), where maternal experience significantly increased PNN density in the right hemisphere than the left of WT (NW-L: n = 13 images; NW-R: n = 22 images; SW-L: n = 21 images; SW-R: n = 25 images; 5 mice per condition; *Kruskal-Wallis followed by Dunn's test, ***p < 0.001*).

| Regions | Whole brain | | | | | Left Hemisphere | | | | | Right Hemisphere | | | |
|---|---|---|---|---|---|---|---|---|---|---|---|---|---|---|
| | NW | NH | SW | SH | | NW-L | NH-L | SW-L | SH-L | | NW-R | NH-R | SW-R | SH-R |
| S1BF | 26.6 ± 3.5[e] | 56.0 ± 6.6[e] | 44.4 ± 5.8 | 47.0 ± 5.4 | | 31.7 ± 5.9[f] | 41.0 ± 5.9[f] | 36.1 ± 7.8 | 37.6 ± 5.4 | | 21.4 ± 3.6[g,h] | 72.2 ± 11.9[g] | 52.8 ± 8.4[h] | 56.3 ± 9.3 |
| S1ULp | 28.3 ± 4.8[o] | 47.0 ± 8.1[o] | 37.9 ± 5.7 | 52.9 ± 7.6 | | 33.4 ± 7.3 | 45.3 ± 8.2 | 29.1 ± 6.7 | 44.2 ± 9.7 | | 23.5 ± 6.3 | 49.2 ± 15.2[p] | 38.9 ± 8.0 | 62.5 ± 11.8[p] |
| S1FL | 17.0 ± 5.0 | 20.9 ± 4.0 | 19.8 ± 6.2 | 18.4 ± 3.6 | | 10.6 ± 4.2[s] | 20.8 ± 5.0 | **3.2 ± 1.3[s,t,u]** | **8.1 ± 2.2[t,v]** | | 20.8 ± 7.5 | 21.0 ± 6.4 | **33.8 ± 10.7[u]** | **30.6 ± 6.6[v]** |
| S1J | 2.5 ± 0.8[i] | 4.2 ± 0.9[i] | 6.7 ± 3.6 | 8.4 ± 2.0 | | 4.0 ± 1.6[k] | 5.2 ± 1.4[k,l] | 9.0 ± 6.8 | 3.6 ± 1.2[l] | | 1.3 ± 0.4[m] | 3.0 ± 0.7[m] | 4.2 ± 1.3[n] | 14.0 ± 3.9[n] |
| S1 | 6.5 ± 0.9[a] | 16.7 ± 2.8[a] | 14.4 ± 3.7[b] | 14.4 ± 2.1[b] | | 7.0 ± 1.6 | 11.4 ± 2.5 | 16.7 ± 6.6 | 11.4 ± 2.1 | | 6.0 ± 1.0[c] | 22.5 ± 5.0[c] | 12.3 ± 3.2[d] | 17.5 ± 3.6[d] |
| S1DZ | 5.4 ± 1.7 | 9.1 ± 2.6 | 8.0 ± 2.3 | 12.7 ± 3.5 | | 3.2 ± 2.0 | 7.4 ± 3.4 | **2.8 ± 1.2[q]** | **6.7 ± 4.0[r]** | | 6.6 ± 2.4 | 10.1 ± 3.8 | **13.4 ± 4.3[q]** | **20.6 ± 5.6[r]** |

**Table 1:** Average high-intensity PNN density across subregions and hemispheres of the SS1 before and after maternal behavior experience. NW, NH, SW and SH are the four different conditions. Primary somatosensory cortex subregions: S1BF, S1ULp, S1FL, S1J, S1, and S1DZ. Significant differences are denoted between genotypes by shading (E.g., NW vs NH), between hemispheres of the same condition by **bold** lettering and between Naïves and Surrogates in the same genotype by bolder borders. Each letter pair corresponds to statistically significant differences between two conditions. Numbers correspond to average PNN density with standard error mean across multiple sections. N = 8 – 85 images for hemisphere analysis, 123-168 images for combined hemisphere analysis; 5 mice per condition; *Kruskal-Wallis followed by Dunn's test*.

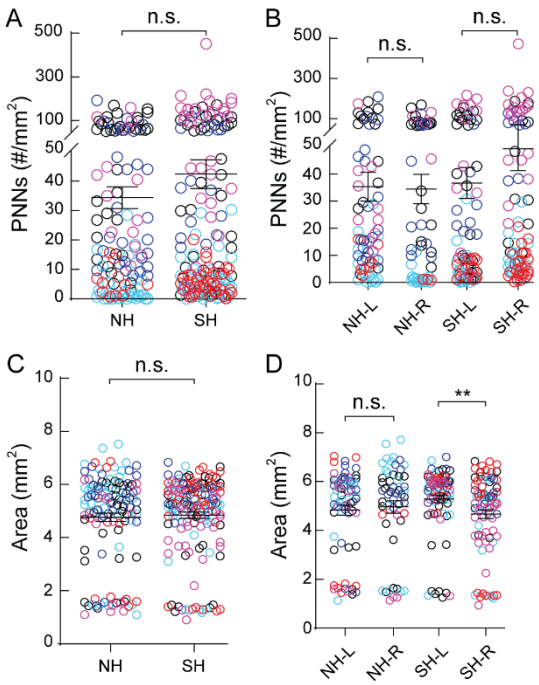


**Figure 4: Hemisphere-specific PNN density changes are not conserved in *Mecp2$^{Het}$* after learned maternal behavior. (A)** Analysis of PNN density in both hemispheres of SS1 did not reveal significant changes between Naïve Het (NH, n = 123 images) and Surrogate Het (SH, n = 162 images) (*Mann-Whitney test, p > 0.05*). **(B)** Analysis of PNN density between hemispheres of SS1 revealed no significant changes after maternal learning (n = 54 – 82 images; *Kruskal-Wallis followed by Dunn's test, p > 0.05*). **(C)** Analysis of SS1 area in both hemispheres revealed no significant changes after maternal learning (NH: n = 123 images; SH: n = 162 images; *Mann-Whitney test, p > 0.05*). **(D)** Area analysis by hemispheres reveal that left hemisphere of SH (SH-L) was significantly larger than the right hemispheres of SH (SH-R). This hemispheric area bias was absent in NH (n = 54 – 82 images; *Kruskal-Wallis followed by Dunn's test, **p < 0.01*). N.s. = not significant. 5 mice per condition.

the right than the left hemisphere for both regions.

For S1BF, a region well-studied for whisker activity that contributes to tactile sensation, PNN density increased significantly and specifically in the right hemisphere for SW, compared to NW (Figure 3A'). This result suggests that increased PNN density in the right hemisphere of S1BF could be a potential site for consolidation of tactile sensory information relevant for executing efficient pup retrieval during the learned maternal behavioral task. Other brain regions (S1ULp, S1J and S1DZ) showed no changes after surrogacy, to further highlight S1BF as a potential site for learning consolidation (Table 1). In analyzing left hemisphere-specific data, there is a decrease in PNN density in S1FL of SW compared to NW (Table 1, columns 5, 7). This is the first report, to our knowledge, of decreases in PNN density in a social behavior context in adult brains. Together, these results suggest that PNN density changes in adult females, in a hemisphere and subregion-specific manner under conducive conditions for experience-dependent plasticity.

**Appropriate PNN expression in SS1 is dependent on MECP2:**

Methyl-CpG-binding protein 2 (MECP2) is thought to regulate experience-dependent plasticity mechanisms in an epigenetic manner, in early postnatal development and in adulthood (Cohen et al., 2011b; Dani et al., 2005; Durand et al., 2012; Gabel et al., 2015; Guy et al., 2001; Krishnan et al., 2015, 2017; Lagger et al., 2017; Morello et al., 2018; Muotri et al., 2010; Noutel et al., 2011; Picard and Fagiolini, 2019). We previously tested this hypothesis, using the learned maternal behavior paradigm, and found that Mecp2-heterozygous (Het) adult females were inefficient at pup retrieval (Krishnan, Lau et al., 2017). In this study, we identified atypical and transient increases in PNN density in the auditory cortex of Surrogate Het (SH), leading to altered responses of PV+ neurons to auditory cues in SH (Lau et al., 2019). Here, we sought to determine if SS1 of SH exhibited similar alterations in PNN density in subregion specific ways. Comparing Naïve Het (NH) to SH, we noticed no significant differences in PNN density in whole SS1 (Figure 4A, similar to WT in Figure 1E), or within hemispheres of SS1 (Figure 4B, unlike WT in Figure 1F), or across the lateral-medial axis (Figure 5). There were no significant changes in SS1 area between NH and SH (Figure 4C). However, a hemisphere-specific area in SH was noted (Figure 4D).

When we compared PNN density between genotypes, WT and Het (Table 1), we noticed significant hemisphere-specific and subregion-specific differences. In general, NH had increased PNN density over NW across subregions; and largely no significant differences after surrogacy (SW vs. SH), except for S1 (which show statistical significance, though mean PNN density is similar. This is likely due to differential distribution of PNN density (Supplemental Figure 1).

In the left hemisphere, there were significant differences between conditions, genotypes and subregions. NH had increased PNN density in S1BF and S1J, compared to NW (Table 1, columns 5,

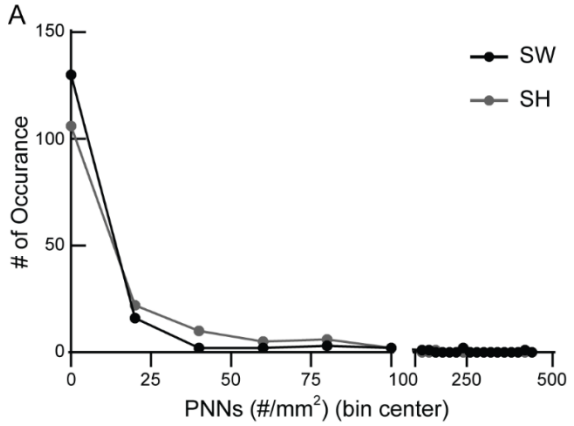


**Supplemental Figure 1: Significant difference in S1 PNN density between SH and SW is explained by differential distribution of data. (A)** Histogram analysis shows that SW had more occurrences of 0 PNN density, compared to SH, as shown by black dot above grey dot. SH had more occurrences of 20-80 PNN density values than SW, as shown by grey dots above black dots. The average PNN density values of SW (n = 160 images) and SH (n = 152 images) are similar (Table 1) (5 mice per condition), but they are statistically different due to this differential distribution of data.

6). SH had increased PNN density in only S1FL, compared to SW (Table 1, columns 7, 8). In the right hemisphere, NH had increased PNN density in S1BF, S1J and S1, compared to NW. SH had increased PNN density in S1J and S1, compared to SW. Surrogacy correlated with increased PNN density in only S1BF of WT (NW vs. SW) (also Fig 1F), while the same increase was not seen in Het (NH vs. SH), with NH-R already exhibiting high PNN density. Interestingly, S1ULp showed increased PNN density in SH-R compared to NH-R (Table 1, columns 10, 12), while a similar result was not observed in WT.

Comparing the hemispheres within genotypes, NW and NH did not have significant differences in PNN density in subregions. However, after learned maternal behavior experience, PNN density increased in the right hemisphere of S1FL and S1DZ in both SW and SH (Table 1), suggesting preserved common experience-dependent plasticity mechanism activation in these regions within the right hemisphere.

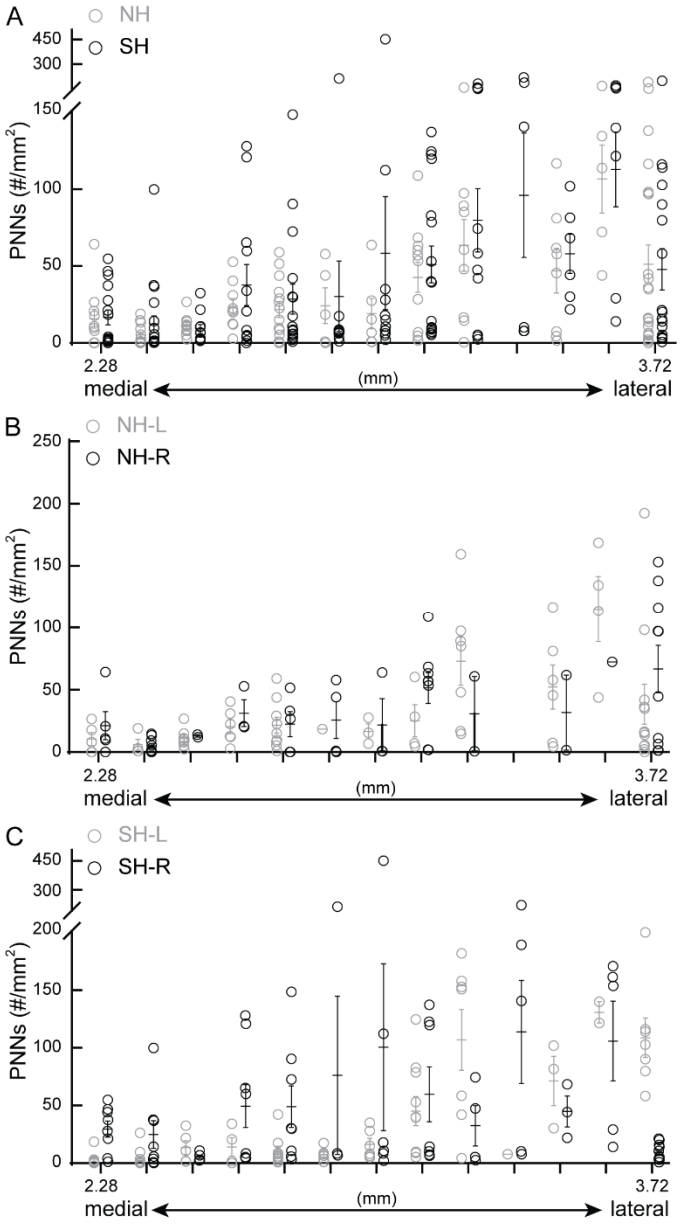


**Figure 5: Overall patterns of PNN density across medial/lateral axis is preserved in *Mecp2$^{Het}$*. (A)** Mean distribution of combined PNN density revealed a gradual increase of PNN density from medial (starting at 2.28 mm) to lateral (ends at 3.72 mm) SS1 in NH. SH exhibited increased PNN density throughout SS1. N = 5 – 22 images per region, 5 mice per condition. **(B)** In NH, the mean distribution of PNN density was similar between left and right hemispheres throughout SS1, with the exception of more lateral regions. **(C)** SH exhibited dynamic changes in PNN density between left and right hemispheres as well as throughout medial and lateral SS1. For A-C, mean ± S.E.M. are shown. Each dot represents PNN density in an individual section. 5 mice per condition. For B and C, n = 1 – 12 images per map coordinate.

**Principal component analysis identifies lateral-medial and hemisphere-specific changes in PNN expression:**

Due to the increasing number of variables being compared, we chose an unsupervised statistical procedure called principal component analysis (PCA), commonly used in genomics/transcriptomics

analysis, to determine if patterns emerge from the PNN density data. PCA takes a set of measurements across samples and identifies the measurements that best capture the variation between the samples. It results in a set of uncorrelated components (called principal components) that each capture an orthogonal aspect of the differences across the samples. As input to PCA, we used PNN densities

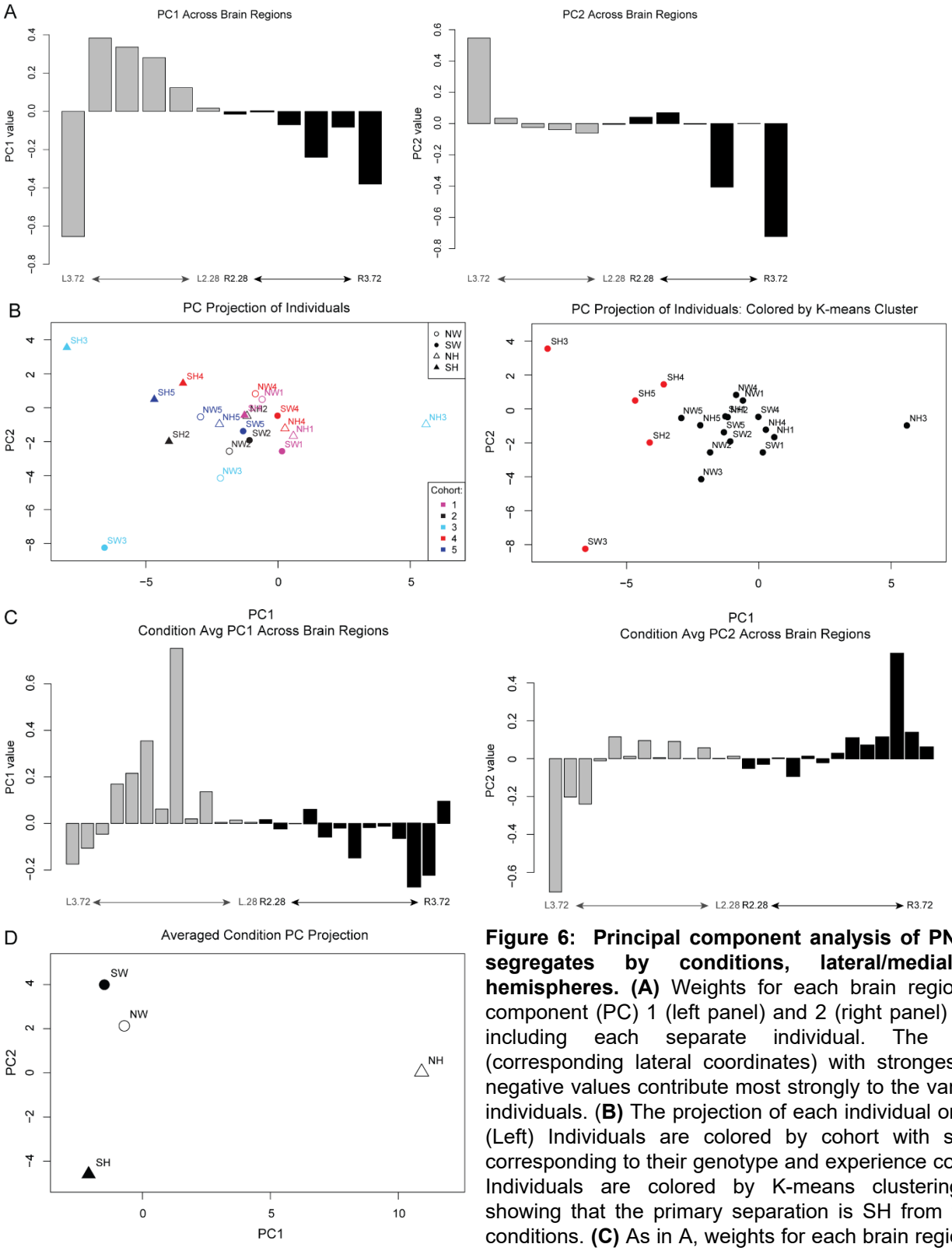


**Figure 6: Principal component analysis of PNN expression segregates by conditions, lateral/medial axis and hemispheres. (A)** Weights for each brain region for principal component (PC) 1 (left panel) and 2 (right panel) in the analysis including each separate individual. The map regions (corresponding lateral coordinates) with strongest positive and negative values contribute most strongly to the variation between individuals. (**B**) The projection of each individual onto PC1 and 2. (Left) Individuals are colored by cohort with symbol shapes corresponding to their genotype and experience condition. (Right) Individuals are colored by K-means clustering assignment, showing that the primary separation is SH from the rest of the conditions. **(C)** As in A, weights for each brain region for PC1 (left panel) and 2 (right panel) are shown, in this case for PCA on data in which all cohorts were averaged for each condition. **(D)** Conditions projected onto PC1 show a separation of NH from the rest while PC2 axis shows a separation of SH from SW.

across individual sections and map numbers (represented as lateral coordinates) across all conditions in the five cohorts. If multiple sections per map number were present, values were averaged across sections to give a single density value.

In the first PCA analysis (Figure 6A, B), we sought to determine whether the PNN patterns segregated primarily by cohort or condition (genotype and experience). We preserved data for each individual brain and averaged PNN densities across every set of 2 adjacent map regions (Figure 6A). By examining the projection of each individual onto the first and second principal components, we found that, while there is biological variability between cohorts, the individuals in a given cohort did not cluster separately from one another in this unsupervised analysis (Fig 6B, left), suggesting that technical variability in processing samples across five cohorts is not the primary driver of PNN density differences. This is an important control to assess technical or biological variability in this data. Instead, the major classification revealed by PCA distinguished the SH PNN density patterns from all others, especially NH (Figure 6B, right), and is primarily captured in the first principal component (PC1). The weights of each section in principal component 1 shows a left-right asymmetry and increasing weights for lateral vs. medial sections, confirming our earlier observations.

In the second PCA analysis (Figure 6C, D), we sought to determine the major PNN density patterns that distinguish genotypes and conditions. Instead of averaging map numbers as in the previous analysis, we preserved data for each map number and averaged the median normalized PNN densities across the 5 cohorts for each condition and then performed PCA to determine the major distinguishing patterns. This analysis revealed patterns of PNN density that best distinguish Naïve vs. Surrogate Het (PC1) and Surrogate WT vs. Surrogate Het (PC2) (Figure 6C, D). These PC patterns also reflect the lateral/medial and left/right asymmetries, thus confirming the anatomical and neurobiological distinctions in the previous figures. Overall, we observe that unsupervised analysis identifies these lateral/medial and left/right asymmetries as the major pattern that characterizes the differences in PNN distribution between experience and genotype.

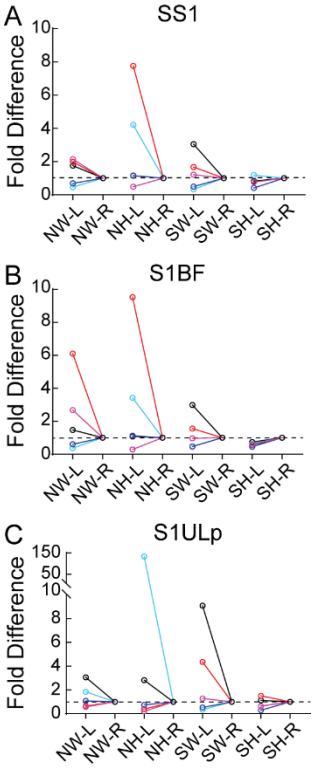


**Figure 7: Individual mouse exhibits hemispheric bias for PNN density. (A-C)** For each mouse, PNN density from the left hemisphere was normalized to the right hemisphere. This left-right hemisphere normalization revealed varying patterns of dominance. **(A)** In SS1, three NW mice exhibit left hemisphere bias of 2-fold, while two mice have a slight right bias (blue colors). After surrogacy, left hemisphere bias is increased to 4-fold in one mouse (black circle), while others remain similar to NW levels. Two NHs exhibit large fold differences favoring left hemisphere (red, blue circles). After surrogacy, dramatic loss in hemispheric bias is observed in the five mice brains. Similar trends with larger fold differences are seen in S1BF **(B)** and S1ULp **(C)**.

**Strong laterality in individual mice brains:**

As the previous data were an aggregate/average of five biological replicates, we were interested in determining if hemispheric biases in PNN density were seen in individual mice. We normalized PNN density of left and right hemisphere per animal (Figure 7). In SS1 as a whole, a modest left hemisphere bias was seen in three out of five mice across conditions and genotypes (Figure 7A). Higher differences in left hemisphere bias is seen in subregions such as S1BF (Figure 7B) and S1ULp (Figure 7C). Interestingly, a decrease in the left hemisphere bias is observed in most of the SH mice. Together, these results show that individual mice have differing hemispheric bias in PNN density in SS1,

which may contribute to individual variability in learning and consolidating new tasks involving tactile sensation.

**Discussion:**

Given the long-standing and revitalized interest in extracellular matrix structures in the brain, we sought to systematically characterize high-intensity PNN expression in the whole SS1 in a model of adult experience-dependent plasticity, in relevant social behavioral conditions. To our knowledge, this is the first systematic characterization of PNN expression in the adult primary somatosensory cortex with nuanced information about subregions and hemispheres in individual mice.

In early postnatal cortical development, expression of PNNs increases progressively with the maturation of that network. An excellent example is the primary visual cortex where the developmental increase of PNNs is regulated by visual experience (Beurdeley et al., 2012; Hou et al., 2017). PNNs in mature primary visual cortex mainly surround the soma and proximal dendrites of PV+ interneurons (Celio, 1993; Hartig et al., 1992; Ueno et al., 2018). Mature PNNs are thought to be inhibitory for experience-dependent plasticity, as their increase in developing primary visual cortex correlates with the termination of the critical period and PNN removal in adult primary visual cortex restores plasticity, as measured by ocular dominance plasticity assays (Bavelier et al., 2010; Pizzorusso et al., 2002, 2006). These and studies in other brain regions (amygdala, hippocampus, piriform & auditory cortex) have suggested that PNNs are stable, long-term structures (Miyata and Kitagawa, 2017; Sorg et al., 2016; Ueno et al., 2019). Experiments involving the enzymatic removal of PNN by chondroitinase ABC or hyaluronidase injections in amygdala, hippocampus, piriform and auditory cortices have shown that synaptic plasticity can be reactivated (Banerjee et al., 2017; Gogolla et al., 2009; Kochlamazashvili et al., 2010; Krishnan, Lau et al., 2017; Pizzorusso et al., 2002; Thompson et al., 2018). Our current study, on the other hand, shows that PNNs are dynamic structures in adulthood under socially relevant behavioral conditions.

What governs PNN dynamics in adults? Matrix metallopeptides and proteases are known to assist in remodeling extracellular matrix structures (Lorenzo Bozzelli et al., 2018; Lu et al., 2011; Miyata and Kitagawa, 2017). However, the contexts and mechanisms for inducing remodeling in adult brains are currently unclear. Some regional and temporal changes in PNN density have been described before (Ueno et al., 2018, 2019). However, systematic, finer scale whole-brain analysis of WFA expression across entire brain regions during development and adulthood has not been performed. Our study suggests PNNs, as measured by WFA immunostaining, may not be stable and static structures as once thought. In this study, we show that high-intensity PNNs of SS1 exhibit increased and decreased expression in a subregion-specific, hemisphere-specific manner, after maternal behavior experience. Currently, these differences in PNN expression between Naïves and Surrogates occur over one-two weeks (three – five days before pups are born plus six days of behavior before perfusions). The rate of PNN formation and remodeling, which might ultimately affect tactile perception and efficient pup retrieval, remains unknown.

In the Paxinos and Franklin atlas, anatomical subregions were classified based on structural connectivity studies. Based on these anatomical characterizations, we speculate that changes in PNN density in specific subregions could impact information processing. For example, when NW female mice learn maternal behavior to become surrogates, there is an increase in PNN density in the right S1BF, and a concomitant decrease in left S1FL (Figure 8), suggesting that these changes contribute to solidifying new synaptic contacts in S1BF, while promoting remodeling in S1FL. Together, these changes could ultimately help process new tactile information related to pups and the mother acquired by the whiskers and forelimbs. Furthermore, right hemisphere-specific PNN increases in S1FL and S1DZ suggests specific rewiring in subregions that could contribute to efficient information processing associated with laterality and dominant hemispheres (Figure 8).

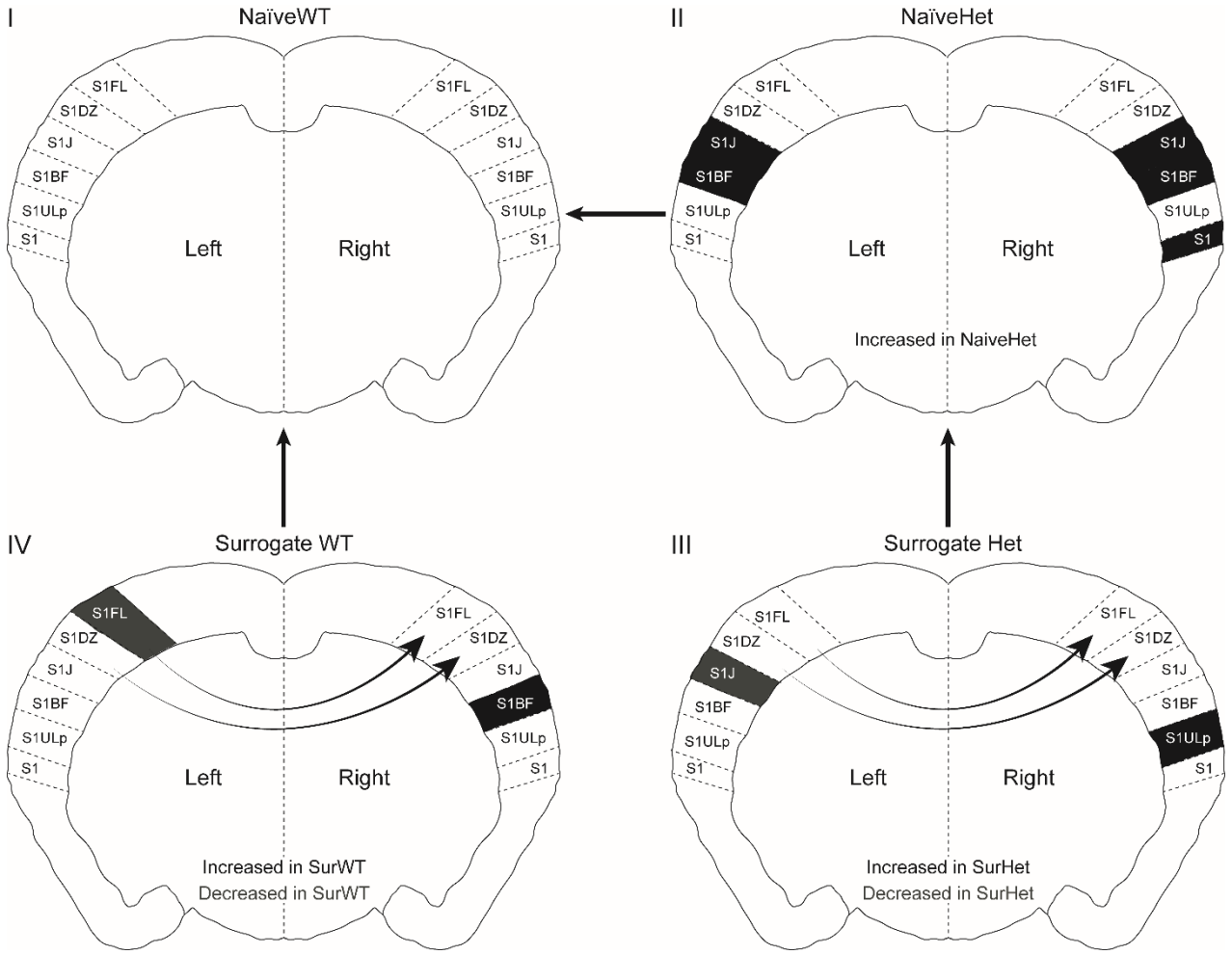


**Figure 8: Summary of changes in PNN density between genotypes in maternal behavior context. (Quadrants I-IV)** The changes in PNN density (grey and black shading) marked inside the brain slices denote comparisons between conditions connected by arrows between brain schemas. Arrows inside the brain schemas indicate hemispheric differences within genotype, with arrowheads pointing to the hemisphere with the higher PNN density. (IV→I) Comparing NW to SW, PNN density is increased in right S1BF and decreased in left S1FL regions of SW. Within SW, PNN density is increased in the right hemisphere, particularly in S1FL and S1DZ. Taken together, PNN density changes in these particular subregions could contribute to tactile perception in SW, ultimately leading to efficient pup retrieval. (II→I) NH had increased PNN density in specific subregions, compared to the NW, suggesting possible tactile perception issues before maternal behavior experience, which could contribute to their inefficient pup retrieval performance. (III→II) SH has increased PNN density in the right S1ULp and decreased density in left S1J, compared to NH, suggesting possible compensatory plasticity mechanisms after maternal experience in Het. SH also displays increased right hemisphere PNN density increases in S1FL and S1DZ, similar to SW, suggesting that right hemisphere-specific increases in PNNs in S1FL and S1DZ might be important for processing tactile information during pup retrieval task.

Previously we showed that, in this adult female mouse model for Rett Syndrome, PNNs were increased in a transient atypical manner in the auditory cortex, which correlated with their inefficient pup retrieval (Krishnan, Lau et al., 2017). Manipulating auditory cortex PNNs by chondriotinase injections or genetic reductions in MECP2 significantly improved aspects of SH pup retrieval behavior, showing that PNNs play crucial roles in learning and executing this behavior (Krishnan, Lau et al., 2017). Current results suggest information flow, network activation and multisensory integration could be affected in *Mecp2*-heterozygous females, in specific cortical regions such as SS1 and auditory cortex (Krishnan, Lau et al., 2017; Morello et al., 2018). Further whole brain analysis on laterality in PNN density in the auditory cortex is warranted, especially due to reports suggesting left hemisphere-specific neural circuitry activation (Ehret et al., 1987; Marlin et al., 2015; Stiebler et al., 1997). Furthermore, MECP2 regulates tactile perception in SS1 of MECP2-deficient male mice (Orefice et al.,

2016). However, it is currently unknown if PNNs are involved in these particular circuits and/or contribute to the observed tactile phenotypes.

The observed fine-scale changes in PNN expression in the adult primary somatosensory cortex before and after maternal behavior experience suggest specific hypotheses about connectivity and functional changes in subregions, specifically in barrel field and upper lip subregions of both hemispheres. *In vivo* electrophysiological and/or imaging studies, which measure dynamics of neural circuitry activation and processing in intact brains, would help prove these hypotheses.

A word of caution: due to ease of immunostaining with WFA and manipulation experiments with chondroitinase ABC, many studies now employ PNNs as markers for plasticity. Our characterization in adult brains shows that these structures are dynamic; having hemisphere-, subregion- specific expression, hinting at potential neural circuitry mechanisms involving laterality in mice. Systematic and careful analysis must be taken to fully characterize PNN expression in experimental design rather than using standard “representative” sample approaches in immunostaining.

**Author contributions:**

BYBL and KK supervised the project, designed experiments and analyzed data. KK, BYBL, DEL, ME and DF performed the behavior experiments. BYBL, DEL, ME and BE performed sectioning and immunostaining. DEL imaged sections. BYBL, DEL, BE, KR, PS mapped sections to the reference atlas. BYBL, DEL, BE, ME, AK, PS, KR, AC, SHB and SR contributed significantly to manual counting of PNN structures. RPM performed and interpreted PCA analysis. BYBL, DEL, RPM and KK wrote and edited the paper.

**Acknowledgements**:

We would like to thank the following students in helping us get started with this project and for technical contributions: Ashlee Tannehill, Taryn Lester, Ronald Dean Franz, Marty Lay and Simran Dayal. This work was supported by postdoctoral fellowship award to BYBL from RettSyndrome.org, research assistantships to DF, BE, ME, PS from UTK and startup funds to KK from University of Tennessee-Knoxville.

**References:**

Amir, R.E., Van den Veyver, I.B., Wan, M., Tran, C.Q., Francke, U., and Zoghbi, H.Y. (1999). Rett syndrome is caused by mutations in X-linked MECP2, encoding methyl-CpG-binding protein 2. Nat. Genet. *23*, 185–188.

Banerjee, S.B., Gutzeit, V.A., Baman, J., Aoued, H.S., Doshi, N.K., Liu, R.C., and Ressler, K.J. (2017). Perineuronal Nets in the Adult Sensory Cortex Are Necessary for Fear Learning. Neuron *95*, 169-179.e3.

Bartos, M., Vida, I., Frotscher, M., Meyer, A., Monyer, H., Geiger, J.R.P., and Jonas, P. (2002). Fast synaptic inhibition promotes synchronized gamma oscillations in hippocampal interneuron networks. Proc. Natl. Acad. Sci. U.S.A. *99*, 13222–13227.

Bavelier, D., Levi, D.M., Li, R.W., Dan, Y., and Hensch, T.K. (2010). Removing Brakes on Adult Brain Plasticity: From Molecular to Behavioral Interventions. Journal of Neuroscience *30*, 14964–14971.

Beach, F.A., and Jaynes, J. (1956). Studies of Maternal Retrieving in Rats. III. Sensory Cues Involved in the Lactating Female’s Response To Her Young. Behaviour *10*, 104–124.

Becker, A., Zhang, P., Allmann, L., Meilinger, D., Bertulat, B., Eck, D., Hofstaetter, M., Bartolomei, G., Hottiger, M.O., Schreiber, V., et al. (2016). Poly(ADP-ribosyl)ation of Methyl CpG Binding Domain Protein 2 Regulates Chromatin Structure. Journal of Biological Chemistry *291*, 4873–4881.

Begum, M.R., and Sng, J.C.G. (2017). Molecular mechanisms of experience-dependent maturation in cortical GABAergic inhibition. Journal of Neurochemistry *142*, 649–661.

Bernard, C., and Prochiantz, A. (2016). Otx2-PNN Interaction to Regulate Cortical Plasticity. Neural Plasticity *2016*, 1–7.

Berretta, S., Pantazopoulos, H., Markota, M., Brown, C., and Batzianouli, E.T. (2015). Losing the sugar coating: Potential impact of perineuronal net abnormalities on interneurons in schizophrenia. Schizophrenia Research *167*, 18–27.

Bignami, A., Asher, R., and Perides, G. (1992). Co-localization of hyaluronic acid and chondroitin sulfate proteoglycan in rat cerebral cortex. Brain Res. *579*, 173–177.

Brecht, M. (2007). Barrel cortex and whisker-mediated behaviors. Curr. Opin. Neurobiol. *17*, 408–416.

Brückner, G., Bringmann, A., Köppe, G., Härtig, W., and Brauer, K. (1996). In vivo and in vitro labelling of perineuronal nets in rat brain. Brain Res. *720*, 84–92.

Brückner, G., Morawski, M., and Arendt, T. (2008). Aggrecan-based extracellular matrix is an integral part of the human basal ganglia circuit. Neuroscience *151*, 489–504.

Carstens, K.E., Phillips, M.L., Pozzo-Miller, L., Weinberg, R.J., and Dudek, S.M. (2016). Perineuronal Nets Suppress Plasticity of Excitatory Synapses on CA2 Pyramidal Neurons. The Journal of Neuroscience *36*, 6312–6320.

Carulli, D., Rhodes, K.E., and Fawcett, J.W. (2007). Upregulation of aggrecan, link protein 1, and hyaluronan synthases during formation of perineuronal nets in the rat cerebellum. The Journal of Comparative Neurology *501*, 83–94.

Cattaud, V., Bezzina, C., Rey, C.C., Lejards, C., Dahan, L., and Verret, L. (2018). Early disruption of parvalbumin expression and perineuronal nets in the hippocampus of the Tg2576 mouse model of Alzheimer's disease can be rescued by enriched environment. Neurobiol. Aging *72*, 147–158.

Celio, M.R. (1993). Perineuronal nets of extracellular matrix around parvalbumin-containing neurons of the hippocampus. Hippocampus *3 Spec No*, 55–60.

Chahrour, M., Jung, S.Y., Shaw, C., Zhou, X., Wong, S.T.C., Qin, J., and Zoghbi, H.Y. (2008). MeCP2, a Key Contributor to Neurological Disease, Activates and Represses Transcription. Science *320*, 1224–1229.

Cohen, L., Rothschild, G., and Mizrahi, A. (2011a). Multisensory integration of natural odors and sounds in the auditory cortex. Neuron *72*, 357–369.

Cohen, S., Gabel, H.W., Hemberg, M., Hutchinson, A.N., Sadacca, L.A., Ebert, D.H., Harmin, D.A., Greenberg, R.S., Verdine, V.K., Zhou, Z., et al. (2011b). Genome-wide activity-dependent MeCP2 phosphorylation regulates nervous system development and function. Neuron *72*, 72–85.

Dani, V.S., Chang, Q., Maffei, A., Turrigiano, G.G., Jaenisch, R., and Nelson, S.B. (2005). Reduced cortical activity due to a shift in the balance between excitation and inhibition in a mouse model of Rett syndrome. Proc. Natl. Acad. Sci. U.S.A. *102*, 12560–12565.

Deepa, S.S., Umehara, Y., Higashiyama, S., Itoh, N., and Sugahara, K. (2002). Specific molecular interactions of oversulfated chondroitin sulfate E with various heparin-binding growth factors. Implications as a physiological binding partner in the brain and other tissues. J. Biol. Chem. *277*, 43707–43716.

Dityatev, A., Brückner, G., Dityateva, G., Grosche, J., Kleene, R., and Schachner, M. (2007). Activity-dependent formation and functions of chondroitin sulfate-rich extracellular matrix of perineuronal nets. Developmental Neurobiology *67*, 570–588.

Donato, F., Rompani, S.B., and Caroni, P. (2013). Parvalbumin-expressing basket-cell network plasticity induced by experience regulates adult learning. Nature *504*, 272–276.

Durand, S., Patrizi, A., Quast, K.B., Hachigian, L., Pavlyuk, R., Saxena, A., Carninci, P., Hensch, T.K., and Fagiolini, M. (2012). NMDA receptor regulation prevents regression of visual cortical function in the absence of Mecp2. Neuron *76*, 1078–1090.

Ebert, D.H., Gabel, H.W., Robinson, N.D., Kastan, N.R., Hu, L.S., Cohen, S., Navarro, A.J., Lyst, M.J., Ekiert, R., Bird, A.P., et al. (2013). Activity-dependent phosphorylation of MeCP2 threonine 308 regulates interaction with NCoR. Nature *499*, 341–345.

Ehret, G., Koch, M., Haack, B., and Markl, H. (1987). Sex and parental experience determine the onset of an instinctive behavior in mice. Naturwissenschaften *74*, 47.

Feldman, D.E., and Brecht, M. (2005). Map plasticity in somatosensory cortex. Science *310*, 810–815.

Frischknecht, R., Heine, M., Perrais, D., Seidenbecher, C.I., Choquet, D., and Gundelfinger, E.D. (2009). Brain extracellular matrix affects AMPA receptor lateral mobility and short-term synaptic plasticity. Nat. Neurosci. *12*, 897–904.

Gabel, H.W., Kinde, B., Stroud, H., Gilbert, C.S., Harmin, D.A., Kastan, N.R., Hemberg, M., Ebert, D.H., and Greenberg, M.E. (2015). Disruption of DNA-methylation-dependent long gene repression in Rett syndrome. Nature *522*, 89–93.

Galtrey, C.M., Asher, R.A., Nothias, F., and Fawcett, J.W. (2007). Promoting plasticity in the spinal cord with chondroitinase improves functional recovery after peripheral nerve repair. Brain *130*, 926–939.

Gogolla, N., Caroni, P., Lüthi, A., and Herry, C. (2009). Perineuronal nets protect fear memories from erasure. Science *325*, 1258–1261.

Gundelfinger, E.D., Frischknecht, R., Choquet, D., and Heine, M. (2010). Converting juvenile into adult plasticity: a role for the brain's extracellular matrix: Converting juvenile into adult plasticity. European Journal of Neuroscience *31*, 2156–2165.

Guy, J., Hendrich, B., Holmes, M., Martin, J.E., and Bird, A. (2001). A mouse Mecp2-null mutation causes neurological symptoms that mimic Rett syndrome. Nat. Genet. *27*, 322–326.

Hartig, W., Brauer, K., and Bruckner, G. (1992). Wisteria floribunda agglutinin-labelled nets surround parvalbumin-containing neurons. Neuroreport *3*, 869–872.

Hou, X., Yoshioka, N., Tsukano, H., Sakai, A., Miyata, S., Watanabe, Y., Yanagawa, Y., Sakimura, K., Takeuchi, K., Kitagawa, H., et al. (2017). Chondroitin Sulfate Is Required for Onset and Offset of Critical Period Plasticity in Visual Cortex. Scientific Reports *7*.

Kalemaki, K., Konstantoudaki, X., Tivodar, S., Sidiropoulou, K., and Karagogeos, D. (2018). Mice With Decreased Number of Interneurons Exhibit Aberrant Spontaneous and Oscillatory Activity in the Cortex. Frontiers in Neural Circuits *12*.

Kenyon, P., Cronin, P., and Keeble, S. (1981). Disruption of maternal retrieving by perioral anesthesia. Physiology & Behavior *27*, 313–321.

Kochlamazashvili, G., Henneberger, C., Bukalo, O., Dvoretskova, E., Senkov, O., Lievens, P.M.-J., Westenbroek, R., Engel, A.K., Catterall, W.A., Rusakov, D.A., et al. (2010). The Extracellular Matrix Molecule Hyaluronic Acid Regulates Hippocampal Synaptic Plasticity by Modulating Postsynaptic L-Type Ca2+ Channels. Neuron *67*, 116–128.

Kosaka, T., and Heizmann, C.W. (1989). Selective staining of a population of parvalbumin-containing GABAergic neurons in the rat cerebral cortex by lectins with specific affinity for terminal N-acetylgalactosamine. Brain Res. *483*, 158–163.

Krishnan, K., Wang, B.S., Lu, J., Wang, L., Maffei, A., Cang, J., and Huang, Z.J. (2015). MeCP2 regulates the timing of critical period plasticity that shapes functional connectivity in primary visual cortex. Proceedings of the National Academy of Sciences of the United States of America *112*, E4782-91.

Krishnan, K., Lau, B.Y.B., Ewall, G., Huang, Z.J., and Shea, S.D. (2017). MECP2 regulates cortical plasticity underlying a learned behaviour in adult female mice. Nature Communications *8*, 14077.

Kwok, J.C.F., Carulli, D., and Fawcett, J.W. (2010). In vitro modeling of perineuronal nets: hyaluronan synthase and link protein are necessary for their formation and integrity: Hyaluronan synthase and link protein in PNNs. Journal of Neurochemistry no-no.

Lagger, S., Connelly, J.C., Schweikert, G., Webb, S., Selfridge, J., Ramsahoye, B.H., Yu, M., He, C., Sanguinetti, G., Sowers, L.C., et al. (2017). MeCP2 recognizes cytosine methylated tri-nucleotide and di-nucleotide sequences to tune transcription in the mammalian brain. PLoS Genet *13*.

Lau, B.Y.B., Krishnan, K., Huang, Z.J., and Shea, S.D. (2019). Maternal experience-dependent cortical plasticity in mice is circuit- and stimulus-specific and requires MECP2. BioRxiv. doi:https://doi.org/10.1101/655035

Lonstein, J.S., Lévy, F., and Fleming, A.S. (2015). Common and divergent psychobiological mechanisms underlying maternal behaviors in non-human and human mammals. Hormones and Behavior *73*, 156–185.

Lorenzo Bozzelli, P., Alaiyed, S., Kim, E., Villapol, S., and Conant, K. (2018). Proteolytic Remodeling of Perineuronal Nets: Effects on Synaptic Plasticity and Neuronal Population Dynamics. Neural Plasticity *2018*, 5735789.

Lu, P., Takai, K., Weaver, V.M., and Werb, Z. (2011). Extracellular Matrix Degradation and Remodeling in Development and Disease. Cold Spring Harbor Perspectives in Biology *3*, a005058–a005058.

Marlin, B.J., Mitre, M., D'amour, J.A., Chao, M.V., and Froemke, R.C. (2015). Oxytocin enables maternal behaviour by balancing cortical inhibition. Nature *520*, 499–504.

Miyata, S., and Kitagawa, H. (2017). Formation and remodeling of the brain extracellular matrix in neural plasticity: Roles of chondroitin sulfate and hyaluronan. Biochimica et Biophysica Acta *1861*, 2420–2434.

Miyata, S., Komatsu, Y., Yoshimura, Y., Taya, C., and Kitagawa, H. (2012). Persistent cortical plasticity by upregulation of chondroitin 6-sulfation. Nat. Neurosci. *15*, 414–422, S1-2.

Morawski, M., Brückner, M.K., Riederer, P., Brückner, G., and Arendt, T. (2004). Perineuronal nets potentially protect against oxidative stress. Exp. Neurol. *188*, 309–315.

Morello, N., Schina, R., Pilotto, F., Phillips, M., Melani, R., Plicato, O., Pizzorusso, T., Pozzo-Miller, L., and Giustetto, M. (2018). Loss of Mecp2 Causes Atypical Synaptic and Molecular Plasticity of Parvalbumin-Expressing Interneurons Reflecting Rett Syndrome–Like Sensorimotor Defects. Eneuro *5*, ENEURO.0086-18.2018.

Morgan, H.D., Fleming, A.S., and Stern, J.M. (1992). Somatosensory control of the onset and retention of maternal responsiveness in primiparous Sprague-Dawley rats. Physiology & Behavior *51*, 549–555.

Muotri, A.R., Marchetto, M.C.N., Coufal, N.G., Oefner, R., Yeo, G., Nakashima, K., and Gage, F.H. (2010). L1 retrotransposition in neurons is modulated by MeCP2. Nature *468*, 443–446.

Murthy, S., Kane, G.A., Katchur, N.J., Lara Mejia, P.S., Obiofuma, G., Buschman, T.J., McEwen, B.S., and Gould, E. (2019). Perineuronal Nets, Inhibitory Interneurons, and Anxiety-Related Ventral Hippocampal Neuronal Oscillations Are Altered by Early Life Adversity. Biol. Psychiatry *85*, 1011–1020.

Nakagawa, F., Schulte, B.A., Wu, J.Y., and Spicer, S.S. (1986). GABAergic neurons of rodent brain correspond partially with those staining for glycoconjugate with terminal N-acetylgalactosamine. J. Neurocytol. *15*, 389–396.

Noutel, J., Hong, Y.K., Leu, B., Kang, E., and Chen, C. (2011). Experience-dependent retinogeniculate synapse remodeling is abnormal in MeCP2-deficient mice. Neuron *70*, 35–42.

Orefice, L.L., Zimmerman, A.L., Chirila, A.M., Sleboda, S.J., Head, J.P., and Ginty, D.D. (2016). Peripheral Mechanosensory Neuron Dysfunction Underlies Tactile and Behavioral Deficits in Mouse Models of ASDs. Cell *166*, 299–313.

Orlando, C., Ster, J., Gerber, U., Fawcett, J.W., and Raineteau, O. (2012). Perisynaptic Chondroitin Sulfate Proteoglycans Restrict Structural Plasticity in an Integrin-Dependent Manner. Journal of Neuroscience *32*, 18009–18017.

Paxinos, G., and Franklin, K.B.J. (2013). Paxino's and Franklin's The Mouse Brain In Stereotaxic Coordinates, 4th Ed (Waltham, MA: Academic Press).

Picard, N., and Fagiolini, M. (2019). MeCP2: an epigenetic regulator of critical periods. Curr. Opin. Neurobiol. *59*, 95–101.

Pizzo, R., Gurgone, A., Castroflorio, E., Amendola, E., Gross, C., Sassoè-Pognetto, M., and Giustetto, M. (2016). Lack of Cdkl5 Disrupts the Organization of Excitatory and Inhibitory Synapses and Parvalbumin Interneurons in the Primary Visual Cortex. Front Cell Neurosci *10*, 261.

Pizzorusso, T., Medini, P., Berardi, N., Chierzi, S., Fawcett, J.W., and Maffei, L. (2002). Reactivation of ocular dominance plasticity in the adult visual cortex. Science *298*, 1248–1251.

Pizzorusso, T., Medini, P., Landi, S., Baldini, S., Berardi, N., and Maffei, L. (2006). Structural and functional recovery from early monocular deprivation in adult rats. Proceedings of the National Academy of Sciences *103*, 8517–8522.

Reinhard, S.M., Rais, M., Afroz, S., Hanania, Y., Pendi, K., Espinoza, K., Rosenthal, R., Binder, D.K., Ethell, I.M., and Razak, K.A. (2019). Reduced perineuronal net expression in Fmr1 KO mice auditory cortex and amygdala is linked to impaired fear-associated memory. Neurobiol Learn Mem *164*, 107042.

Schneider, C.A., Rasband, W.S., and Eliceiri, K.W. (2012). NIH Image to ImageJ: 25 years of image analysis. Nat. Methods *9*, 671–675.

Sigal, Y.M., Bae, H., Bogart, L.J., Hensch, T.K., and Zhuang, X. (2019). Structural maturation of cortical perineuronal nets and their perforating synapses revealed by superresolution imaging. Proc. Natl. Acad. Sci. U.S.A. *116*, 7071–7076.

Skene, P.J., Illingworth, R.S., Webb, S., Kerr, A.R.W., James, K.D., Turner, D.J., Andrews, R., and Bird, A.P. (2010). Neuronal MeCP2 Is Expressed at Near Histone-Octamer Levels and Globally Alters the Chromatin State. Molecular Cell *37*, 457–468.

Sorg, B.A., Berretta, S., Blacktop, J.M., Fawcett, J.W., Kitagawa, H., Kwok, J.C.F., and Miquel, M. (2016). Casting a Wide Net: Role of Perineuronal Nets in Neural Plasticity. The Journal of Neuroscience *36*, 11459–11468.

Stern, J.M. (1996). Somatosensation and Maternal Care in Norway Rats. In Advances in the Study of Behavior, (Elsevier), pp. 243–294.

Stiebler, I., Neulist, R., Fichtel, I., and Ehret, G. (1997). The auditory cortex of the house mouse: left-right differences, tonotopic organization and quantitative analysis of frequency representation. J. Comp. Physiol. A *181*, 559–571.

Stolzenberg, D.S., and Champagne, F.A. (2016). Hormonal and non-hormonal bases of maternal behavior: The role of experience and epigenetic mechanisms. Horm Behav *77*, 204–210.

Sugiyama, S., Prochiantz, A., and Hensch, T.K. (2009). From brain formation to plasticity: Insights on Otx2 homeoprotein: Otx2 transfer shapes postnatal circuits. Development, Growth & Differentiation *51*, 369–377.

Suttkus, A., Rohn, S., Jäger, C., Arendt, T., and Morawski, M. (2012). Neuroprotection against iron-induced cell death by perineuronal nets - an in vivo analysis of oxidative stress. Am J Neurodegener Dis *1*, 122–129.

Thompson, E.H., Lensjø, K.K., Wigestrand, M.B., Malthe-Sørenssen, A., Hafting, T., and Fyhn, M. (2018). Removal of perineuronal nets disrupts recall of a remote fear memory. Proceedings of the National Academy of Sciences *115*, 607–612.

Ueno, H., Takao, K., Suemitsu, S., Murakami, S., Kitamura, N., Wani, K., Okamoto, M., Aoki, S., and Ishihara, T. (2018). Age-dependent and region-specific alteration of parvalbumin neurons and perineuronal nets in the mouse cerebral cortex. Neurochemistry International *112*, 59–70.

Ueno, H., Suemitsu, S., Murakami, S., Kitamura, N., Wani, K., Matsumoto, Y., Okamoto, M., and Ishihara, T. (2019). Layer-specific expression of extracellular matrix molecules in the mouse somatosensory and piriform cortices. IBRO Reports *6*, 1–17.

Vo, T., Carulli, D., Ehlert, E.M.E., Kwok, J.C.F., Dick, G., Mecollari, V., Moloney, E.B., Neufeld, G., de Winter, F., Fawcett, J.W., et al. (2013). The chemorepulsive axon guidance protein semaphorin3A is a constituent of perineuronal nets in the adult rodent brain. Molecular and Cellular Neuroscience *56*, 186–200.

de Winter, F., Kwok, J.C.F., Fawcett, J.W., Vo, T.T., Carulli, D., and Verhaagen, J. (2016). The Chemorepulsive Protein Semaphorin 3A and Perineuronal Net-Mediated Plasticity. Neural Plasticity *2016*, 1–14.

Ye, Q., and Miao, Q. (2013). Experience-dependent development of perineuronal nets and chondroitin sulfate proteoglycan receptors in mouse visual cortex. Matrix Biology *32*, 352–363.

Zhou, Z., Hong, E.J., Cohen, S., Zhao, W., Ho, H.H., Schmidt, L., Chen, W.G., Lin, Y., Savner, E., Griffith, E.C., et al. (2006). Brain-Specific Phosphorylation of MeCP2 Regulates Activity-Dependent Bdnf Transcription, Dendritic Growth, and Spine Maturation. Neuron *52*, 255–269.